35th Annual International Conference of the IEEE EMBS
Osaka, Japan, 3 - 7 July, 2013

Scleroderma Capillary Pattern Identification using Texture Descriptors and Ensemble Classification

Gerald Schaefer, Bartosz Krawczyk, Niraj P. Doshi, and Arcangelo Merla

Abstract— **Various connective tissue diseases lead to morphological alternations of blood capillaries. Consequently, observation of the capillaries at the finger nailfold – nailfold capillaroscopy (NC) – is a standard method for diagnosing diseases such as scleroderma or Raynaud's phenomenon. This is typically performed through manual inspection by an expert to lead to a determination of one of the established NC scleroderma patterns (early, active, and late). In this paper, we present an automated method of analysing nailfold capillaroscopy images and categorising them into NC patterns. For this purpose, we extract a carefully chosen set of texture features from the images and employ an ensemble classification approach to arrive at decisions for each captured finger which are then aggregated to form a diagnosis for the patient. Experimental results on a set of 60 NC images from 16 subjects demonstrate the accuracy and usefulness of our presented approach.**

I. Introduction

Nailfold capillaroscopy (NC) is a non-invasive imaging technique employed to assess the condition of blood capillaries in the nailfold, and is recognised as a realiable and affordable method for observing micro blood vessel characteristics as well as a standard method for diagnosing diseases such as systemic sclerosis (SSc) [1], Raynaud's phenomenon [2], and other connective tissue diseases such as dermatomyositis, antiphospholipid syndrome [3], and Sjögren's syndrome [4] which lead to morphological alterations of capillaries.

Such morphological changes include enlarged and giant capillaries, haemorrhages, loss of capillaries, disorganisation of the vascular array, and bushy capillaries [5]. Patterns observable in NC images of SSc patients have been described in [6], and refined into early, active and late patterns in [7], and are also observed in other closely related disorders such as dermatomyositis or mixed connective tissue diseases.

The three NC patterns can be characterised as follows [8] (see also Fig. 1 for examples):

- **Early (E):** few giant capillaries, few capillary haemorrhages, relatively well preserved capillary distribution, no evidence of loss of capillaries.
- **Active (A):** frequent giant capillaries, frequent capillary haemorrhages, moderate loss of capillaries with some avascular areas, mild disorganisation of the capillary architecture, absent or some ramified capillaries.
- **Late (L):** irregular enlargement of the capillaries, few or absent giant capillaries, absence of haemorrhages, severe loss of capillaries with large avascular areas, severe disorganisation of the normal capillary array, frequent ramified/bushy capillaries.

Scleroderma NC patterns are also used to evaluate other rheumatic diseases. For example, scleroderma patterns are often present in dermatositis/polymyositis and are also found among patients suffering from Raynaud's phenomenon and undifferentiated connective tissue diseases [9].

Identification of NC patterns is performed manually by an expert based on visual inspection of the captured NC images, typically of images taken from different fingers. In this paper, we present an automated approach for determining scleroderma patterns from NC images. For this purpose, we extract a set of texture descriptors from the images and employ an ensemble classifier, generated by building multiple support vector machines (derived from different feature spaces obtained by applying different feature selection algorithms) and combining their results using a neural network fuser. Decisions for individual fingers are then aggregated to form a final diagnosis. Experimental results on a set of 60 NC images from 16 subjects demonstrate the accuracy and usefulness of our presented approach.

II. Image Analysis

A. Pre-processing

Automated analysis of NC images is challenging due to various factors including image noise, dust on lenses, micromotion of fingers, and air bubbles in the immersion oil. A first step is therefore to remove noise and enhance the images. In previous work [10], [11] we have performed an extensive evaluation of a variety of denoising and enhancement algorithms on NC images and consequently apply a bilateral enhancer [12] on the captured images.

The bilateral enhancer is based on the bilateral filter [13], a non-iterative, relatively simple algorithm which smoothens an image while preserving edges by means of a non-linear combination of nearby image values based on both their spatial closeness $c(\xi, x)$ and their photometric similarity $s(f(\xi), f(x))$. Bilateral filtering is defined as

$$h(x) = \frac{\int_{\Omega(x)} f(\xi) c(\xi, x) s(f(\xi), f(x)) d\xi}{\int_{\Omega(x)} c(\xi, x) s(f(\xi), f(x)) d\xi}. \quad (1)$$

The bilateral enhancer [12] extends this concept so that edge preserving smoothing and selective sharpening is performed simultaneously. A weighted average is utilised that

G. Schaefer (gerald.schaefer@ieee.org) and N.P. Doshi (n.doshi@lboro.ac.uk) are with the Department of Computer Science, Loughborough University, U.K.

B. Krawczyk (bartosz.krawczyk@pwr.wroc.pl) is with the Department of Systems & Computer Networks, Wrocław University of Technology, Wrocław, Poland.

A. Merla (a.merla@itab.unich.it) is with the Institute of Advanced Biomedical Technologies, Department of Neurosciences and Imaging, University of Chieti-Pescara, Italy.

978-1-4577-0216-7/13/$26.00 ©2013 IEEE

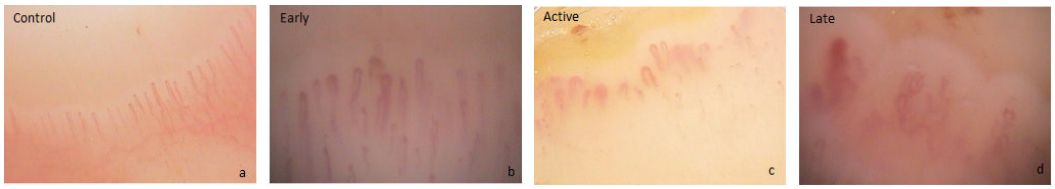

Fig. 1. Examples of scleroderma patterns: (a) healthy subject; (b) early; (c) active; (d) late.

is independent of the design of $c(.)$ and $s(.)$ in Eq. (1). The bilateral enhancer is defined as

$$j(x) = gf(x) + \int_{\frac{\Omega(x)}{x}} c(\xi, x)p(f(x), f(\xi))d\xi, \qquad (2)$$

where $g = c(x, x)s(f(x), f(x))$.

B. Texture analysis

In the few works that attempt to perform automated analysis of NC images [14], [15], [16], [17], [18] single capillaries are extracted and their layout and shapes used for pattern classification. In this paper, we follow a different approach. Not only is exact extraction of capillaries difficult due to the relatively poor image quality (even after enhancement), looking at the examples of Fig. 1 again we can notice that it is possible to distinguish between the different patterns almost 'at a glance'. We therefore propose to employ global image features for analysing and classifying NC images.

In particular, we extract texture information from the images and use it in a subsequent classification stage to determine the associated scleroderma patterns. While a variety of texture features exist, those based on local binary patterns [19] have been found to provide excellent performance for a variety of tasks, including texture classification [20]. We consequently employ LBP features in our approach, also as we found them to provide better accuracy compared to other features such as Gabor or wavelet descriptors.

LBP describes the local neighbourhood of a pixel and, in its basic form, produces 256 texture patterns based on a 3×3 neighbourhood. Neighbouring pixels are set to 0 and 1 by thresholding them with the centre pixel value. The resulting sequence of 0s and 1s is then known as the local binary pattern and a histogram of these patterns over the whole image is generated. Due to the binary decision making, LBP is inherently invariant to intensity changes and hence more robust that other techniques.

LBP patterns are usually obtained from a circular neighbourhood (where values that do not fall exactly at the centre of pixel are estimated by interpolation), while rotation invariance can be obtained by mapping all possible rotated patterns to the same descriptor. Furthermore, certain patterns are fundamental properties of texture and may thus account for the majority of LBP patterns. To address this, only uniform patterns can be utilised where a uniformity measure is defined by the number of transitions from 0 to 1 or vice versa in the LBP code.

Uniform rotation invariant LBP descriptors are powerful texture features and typically perform well [20], however in preliminary tests we noticed that they did not work as well as we expected for our task at end. After some further investigation, we found that including the intensity variance, which gives an indication of image contrast, leads to a significant performance boost. Intensity variance, defined as

$$VAR_{P,R} = \frac{1}{P}\sum_{p=0}^{P-1}(g_p - \mu)^2, \quad \text{where} \quad \mu = \frac{1}{P}\sum_{p=0}^{P-1} g_p, \quad (3)$$

where R defines a radius and P the number of LBP neighbours, can be incorporated into LBP to generate a joint distribution $LBP_{P,R}/VAR_{P,R}$ and give a texture descriptor that contains local pattern and local contrast information. An alternative is the use of a hybrid scheme, LBP variance (LBPV) [21], which uses globally rotation invariant matching with locally variant LBP texture features, and it is this method that we employ.

In LBPV, $VAR_{P,R}$ is used as an adaptive weight to adjust the contribution of the LBP code in the histogram calculation. LBPV histograms are calculated as

$$LBPV_{P,R}(k) = \sum_{i=1}^{N}\sum_{j=1}^{M} w(LBP_{P,R}(i,j), k), \quad k \in [0, K], \qquad (4)$$

with

$$w(LBP_{P,R}(i,j), k) = \begin{cases} VAR_{P,R}(i,j) & \text{if } LBP_{P,R}(i,j) = k \\ 0 & \text{otherwise} \end{cases}. \qquad (5)$$

III. Pattern Classification

The extracted LBPV texture features then form the basis of a pattern classification stage, where, based on training from known samples, we derive a classifier to identify the scleroderma pattern of an image from its texture characteristics.

Pattern classification is a much explored topic with many different classification algorithms proposed in the literature [22]. Recently, much attention has been devoted to the development of ensemble classifiers, or multiple classifier systems [23]. Consequently, while in earlier work we employed a single classifier [24], in this paper we use an ensemble of classifiers. When focussing solely on a single classifier, we discard the fact that other models may also provide a valuable contribution that could be incorporated into the decision making process. The idea of ensemble classifiers is hence to exploit the strengths and local competencies of a pool of classifiers, while at the same time reducing their individual weaknesses. Consequently, an appropriately constructed combination of several predictors can give better results than any single one of them.

Our proposed classifier system is carefully crafted and consists of three main phases:

1) Creation of a pool of diverse individual classifiers;

2) Pruning the pool by removing redundant predictors;
3) Using a trained fuser based on discriminants to combine the outputs of the classifiers.

In the following, we describe these steps in detail.

A. Classifier pool

Individual classifiers used as base models for the committee play a crucial role in the ensemble design process. These models should be complementary to each other, and thus exhibit both high accuracy and high diversity so that jointly they may outperform any single model from the pool.

It is well known that there is no single optimal approach for feature selection and that consequently results obtained on the basis of different methods may differ significantly. Therefore, instead of using a single feature selection method we employ several of them. We thus generate a diverse pool of classifiers through application of different feature selection algorithms; for L feature selection methods we construct a pool of L individual classifiers $\Pi^{\Psi} = \{\Psi^{(1)}, \Psi^{(2)}, ..., \Psi^{(L)}\}$.

As base classifier, we utilise a support vector machine (SVM) [25] with a radial basis function kernel, trained using the SMO procedure [26], and employing a tuning procedure to obtain optimal cost and kernel parameters. We use eight different feature selection algorithms, namely ReliefF [27], Fast Correlation Based Filter [28], Genetic Wrapper [29], Simulated Annealing Wrapper [29], Forward Selection [29], Backward Selection [29], Quick Branch & Bound [29] and Las Vegas Incremental [29].

B. Ensemble pruning

In ensemble classifier design, not all of the L models in Π^{Ψ} should necessarily be used as ensemble members, since some of them may be redundant and therefore should be discarded. While there are various ways of selecting "valuable" committee members, diversity measures are often considered to be one of the most effective methods [30].

For measuring the diversity of the whole ensemble we use an entropy measure. The highest diversity among classifiers for a particular object $x_j \in X$ is equal to $L/2$ of the votes in x_j with the same value (0 or 1) and the other $L - [L/2]$ with the alternative value. If $l(x_j)$ denotes the number of classifiers that correctly recognise a given sample, entropy-based diversity can be described by

$$E = \frac{1}{N} \sum_{j=1}^{N} \frac{1}{L - [L/2]} min\{l(z_j), L - l(z_j)\}, \qquad (6)$$

with E in $[0; 1]$ where 0 indicates no difference and 1 indicates the highest possible diversity. We perform an exhaustive search to find a pruned pool of K classifiers exhibiting the highest possible diversity.

C. Classifier fusion

For combining the different base classifiers, we employ a trained fuser based on discriminant analysis (as opposed to using the predicted class labels). Assume that we have an ensembe of K classifiers, $\Psi^{(1)}$, $\Psi^{(2)}$, ..., $\Psi^{(K)}$, after the pruning procedure. For a given object $x \in \mathcal{X}$, each individual classifier decides for class $i \in \mathcal{M} = \{1, ..., M\}$ based on the values of discriminants. Let $F^{(l)}(i, x)$ denote a function that is assigned to class i for a given value of x, and that is used by the l-th classifier $\Psi^{(l)}$. The combined classifier Ψ uses the decision rule

$$\Psi(x) = i \quad \text{if} \quad \hat{F}(i, x) = \max_{k \in M} \hat{F}(k, x), \qquad (7)$$

where

$$\hat{F}(i, x) = \sum_{l=1}^{K} w^{(l)}(i) F^{(l)}(i, x) \quad \text{and} \quad \sum_{i=1}^{K} w^{(l)}(i) = 1. \quad (8)$$

The weights can be set dependent on the classifier and class number: weight $w^{(l)}(i)$ is assigned to the *l*-th classifier and the *i*-th class, and given classifier weights assigned to different classes may differ.

The trained fuser we employ is a neural fuser implemented as a one-layer perceptron [31]. The values of support functions given by each of the base classifiers serve as input, while the output is the weighted support for each of the classes. One perceptron fuser is constructed for each of the classes. The perceptron may be trained with any standard procedure used in neural network learning (we use the Quickprop algorithm), and the input weights established during the learning process are then the weights assigned to each of the base classifiers.

D. Patient classification

For NC diagnosis, typically several fingers are inspected as specific NC patterns might not show on every finger. A decision is then made based on all fingers. Based on detection of scleroderma patterns in individual images, a *late* decision is made if at least 2 fingers are classified as late, otherwise an *active* pattern is determined if at least 2 fingers are classified as active. Similarly, an *early* pattern is assigned if at least fingers are classified as early (and no late or active decision has been made).

IV. Experimental Results

We carried out our experiments on a dataset of sixteen subjects with NC images for three to four fingers for each patient. The images (some are shown in Fig. 1) were obtained at the Dermatology Unit, Clinical Hospital of Chieti, following their standard protocol, and using an Olympus SZ40 stereo microscope coupled with an external light source. A ground truth for all patients was also obtained by manual inspection carried out by a consultant. Of the 16 subjects, six were found to show early, six active, and two late patterns; the remaining two were control subjects.

Each image is enhanced using the bilateral enhancer and LBPV texture descriptors ($LBPV^{riu2}_{5,8}$, i.e. rotation invariant uniform mapping at uniformity two) are extracted. For evaluation, we perform standard leave-one-out cross validation (LOOCV) on a patient basis; that is the classifier is trained on all but one subject for which we run the test, and the procedure is repeated for all patients (i.e., 16 times in total).

The obtained results are summarised in Table I where we give both the results of classifying each of the fingers

separately and the overall decision for the patient. From Table I, we can see that in most cases the correct pattern for a finger is identified, namely in 50 of the 60 cases which gives a correct classification of 83.3% on a per finger basis. When aggregating the individual predictions, the correct patient diagnosis is obtained in all but one case (Control 2 which is mistaken as an early patient).

TABLE I
CLASSIFICATION RESULTS. INCORRECT RESULTS ARE BOLDED.

Patient	Finger 1	Finger 2	Finger 3	Finger 4	Patient
Control 1	C	**E**	C	-	C
Control 2	**E**	C	**E**	**E**	**E**
Early 1	E	E	E	E	E
Early 2	E	E	**A**	-	E
Early 3	E	E	E	E	E
Early 4	E	E	E	E	E
Early 5	E	E	E	E	E
Early 6	E	E	E	E	E
Active 1	**E**	A	A	A	A
Active 2	**C**	A	A	A	A
Active 3	A	A	A	A	A
Active 4	A	A	A	A	A
Active 5	A	A	A	-	A
Active 6	A	A	A	-	A
Late 1	**E**	L	L	L	L
Late 2	L	L	**E**	**E**	L

Overall, it is clear that our approach provides excellent performance and hence a useful tool for NC based diagnosis.

V. CONCLUSIONS

In this paper, we have presented an approach to analysing nailfold capillaroscopy images with the aim to autmatically identify scleroderma patterns. For this, we extract a set of texture features from the images and employ an ensemble classifier for decision making. Our approach is shown to work well and to give excellent performance on a test dataset of 60 images from 16 patients. Future work will focus on capturing a larger dataset for evaluation and alternative methods of aggregating individual finger classifications.

REFERENCES

[1] W. Grassi, P. D. Medico, F. Izzo, and C. Cervini, "Microvascular involvement in systemic sclerosis: Capillaroscopic findings," *Seminars in Arthritis and Rheumatism*, vol. 30, no. 6, pp. 397–402, 2001.

[2] M. Cutolo, W. Grassi, and M. Matucci Cerinic, "Raynaud's phenomenon and the role of capillaroscopy," *Arthritis & Rheumatism*, vol. 48, no. 11, pp. 3023–3030, 2003.

[3] M. Cutolo, A. Sulli, M. Secchi, S. Paolino, and C. Pizzorni, "Nailfold capillaroscopy is useful for the diagnosis and follow-up of autoimmune rheumatic diseases. a future tool for the analysis of micro-vascular heart involvement?" *Rheumatology*, vol. 45 Suppl 4, no. ii, pp. iv43–iv46, 2006.

[4] M. Tektonidou, E. Kaskani, F. N. Skopouli, and H. M. Moutsopoulos, "Microvascular abnormalities in Sjgren's syndrome: nailfold capillaroscopy," *Rheumatology*, vol. 38, no. 9, pp. 826–830, 1999.

[5] M. Cutolo, C. Pizzorni, and A. Sulli, "Capillaroscopy," *Best Practice and Research Clinical Rheumatology*, vol. 19, no. 3, pp. 437–452, 2005.

[6] H. Maricq and C. LeRoy, "Patterns of finger capillary abnormalities in connective tissue disease by wide-field microscopy," *Arthritis & Rheumatism*, vol. 16, no. 5, pp. 619–628, 1973.

[7] M. Cutolo, A. Sulli, C. Pizzorni, and S. Accardo, "Nailfold videocapillaroscopy assessment of microvascular damage in systemic sclerosis," *The Journal of Rheumatology*, vol. 27, pp. 155–60, 2000.

[8] ——, "Nailfold videocapillaroscopy assessment of microvascular damage in systemic sclerosis," *The Journal of Rheumatology*, vol. 27, no. 1, pp. 155–160, 2000.

[9] Z. Nagy and L. Czirjk, "Nailfold digital capillaroscopy in 447 patients with connective tissue disease and raynaud's disease," *Journal of the European Academy of Dermatology and Venereology*, vol. 18, no. 1, pp. 62–68, 2004.

[10] N. Doshi, G. Schaefer, and A. Merla, "Enhancement of nailfold capillaroscopy images," in *IEEE-EMBS Int. Conference on Biomedical and Health Informatics*, 2012.

[11] ——, "An evaluation of image enhancement techniques for capillary imaging," in *IEEE Int. Conference on Systems, Man, and Cybernetics*, 2012.

[12] C. Gatta and P. Radeva, "Bilateral enhancers," in *16th IEEE International Conference on Image Processing*, 2009, pp. 3161 –3164.

[13] C. Tomasi and R. Manduchi, "Bilateral filtering for gray and color images," in *6th Int. Conference on Computer Vision*, 1998, pp. 839–846.

[14] H. Kwasnicka, M. Paradowski, and K. Borysewicz, "Capillaroscopy image analysis as an automatic image annotation problem," in *6th Interenational Conference on Computer Information Systems and Industrial Management Applications*, 2007.

[15] C.-H. Wen, W.-D. Liao, and K.-C. Li, "Classification framework for nailfold capillary microscopy images," in *10th IEEE Region Conference TENCON*, 2007, pp. 1–4.

[16] C.-H. Wen, T.-Y. Hsieh, W.-D. Liao, J.-L. Lan, D.-Y. Chen, K.-C. Li, and Y.-T. Tsai, "A novel method for classification of high-resolution nailfold capillary microscopy images," in *1st IEEE International Conference on Ubi-Media Computing*, 2008, pp. 513–518.

[17] M. Paradowski, U. Markowska-Kaczmar, H. Kwasnicka, and K. Borysewicz, "Capillary abnormalities detection using vessel thickness and curvature analysis," in *13th Int. Conference on Knowledge-Based and Intelligent Information and Engineering Systems*, 2009, pp. 151–158.

[18] C.-H. Wen, W.-D. Liao, T.-Y. Hsieh, D.-Y. Chen, J.-L. Lan, and K.-C. Li, "Computer-aided image analysis aids early diagnosis of connective-tissue diseases," in *SPIE Newsroom, Biomedical Optics & Medical Imaging*, 2009.

[19] T. Ojala, M. Pietikainen, and T. Maenpaa, "Multiresolution gray-scale and rotation invariant texture classification with local binary patterns," *IEEE Transactions on Pattern Analysis and Machine Intelligence*, vol. 24, pp. 971–987, 2002.

[20] N. Doshi and G. Schaefer, "A comparative analysis of local binary pattern texture classification," in *Visual Communications and Image Processing*, 2012.

[21] Z. Guo, L. Zhang, and D. Zhang, "Rotation invariant texture classification using LBP variance (LBPV) with global matching," *Pattern Recognition*, vol. 43, no. 3, pp. 706 – 719, 2010.

[22] A. Jain, P. Duin, and M. J., "Statistical pattern recognition: A review," *IEEE Trans. Pattern Analysis and Machine Intelligence*, vol. 22, no. 1, pp. 4–37, 2000.

[23] L. Kuncheva, *Combining pattern classifiers: Methods and algorithms*. Wiley-Interscience, New Jersey, 2004.

[24] N. Doshi, G. Schaefer, and A. Merla, "Nailfold capillaroscopy pattern recognition using texture analysis," in *IEEE-EMBS Int. Conference on Biomedical and Health Informatics*, 2012.

[25] V. N. Vapnik, *Statistical Learning Theory*. John Wiley & Sons, 1998.

[26] J. Platt, "Fast training of support vector machines using sequential minimal optimization," in *Advances in Kernel Methods – Support Vector Learning*, B. Schoelkopf, C. Burges, and A. Smola, Eds. MIT Press, 1998.

[27] L. Yu and H. Liu, "Efficient feature selection via analysis of relevance and redundancy," *Journal of Machine Learning Research*, pp. 1205–1224, 2004.

[28] ——, "Feature selection for high-dimensional data: A fast correlation-based filter solution," in *20th Int. Conference on Machine Learning*, vol. 2, 2003, pp. 856–863.

[29] N. M. Guyon I., Gunn S. and Z. L. (eds), *Feature extraction, foundations and applications*. Springer, 2006.

[30] Y. Bi, "The impact of diversity on the accuracy of evidential classifier ensembles," *International Journal of Approximate Reasoning*, vol. 53, no. 4, pp. 584–607, 2012.

[31] M. Wozniak and M. Zmyslony, "Combining classifiers using trained fuser - analytical and experimental results," *Neural Network World*, vol. 13, no. 7, pp. 925–934, 2010.